ANL-HEP-CP-77-37
June 17, 1977

CONF-770406--2

$K\bar{K}$ AMPLITUDE ANALYSES

D. Cohen

Prepared For

Fifth International Conference
on Experimental Meson Spectroscopy
Northeastern University
Boston, MA
April 1977

UofC-ANA-USERDA

ARGONNE NATIONAL LABORATORY, ARGONNE, ILLINOIS

operated under contract W-31-109-Eng-38 for the
U. S. ENERGY RESEARCH AND DEVELOPMENT ADMINISTRATION

The facilities of Argonne National Laboratory are owned by the United States Government. Under the terms of a contract (W-31-109-Eng-38) between the U. S. Energy Research and Development Administration, Argonne Universities Association and The University of Chicago, the University employs the staff and operates the Laboratory in accordance with policies and programs formulated, approved and reviewed by the Association.

MEMBERS OF ARGONNE UNIVERSITIES ASSOCIATION

The University of Arizona	Kansas State University	The Ohio State University
Carnegie-Mellon University	The University of Kansas	Ohio University
Case Western Reserve University	Loyola University	The Pennsylvania State University
The University of Chicago	Marquette University	Purdue University
University of Cincinnati	Michigan State University	Saint Louis University
Illinois Institute of Technology	The University of Michigan	Southern Illinois University
University of Illinois	University of Minnesota	The University of Texas at Austin
Indiana University	University of Missouri	Washington University
Iowa State University	Northwestern University	Wayne State University
The University of Iowa	University of Notre Dame	The University of Wisconsin

ANL-HEP-CP-77-37
June 17, 1977

$K\bar{K}$ AMPLITUDE ANALYSES*

D. Cohen
Argonne National Laboratory
Argonne, Illinois 60439

ABSTRACT

A review is presented of amplitude analyses of the $K\bar{K}$ system produced in reactions of the type $\pi^{\pm}N \to K\bar{K}N$. These analyses establish the existence of a new S-wave $K\bar{K}$ state at a mass of ~1300 MeV, having isospin 0 and a slow phase variation.

INTRODUCTION

I will discuss the results of three experiments that have studied reactions of the type $\pi^{\pm}N \to K\bar{K}N$ and carried out amplitude analyses of the produced $K\bar{K}$ system. The experiments to be discussed are summarized in Table I.

Table I. $K\bar{K}$ Experiments

Group	Ref.	Technique	Reaction	P_{lab}(GeV/c)	Events
Notre Dame, Argonne	1	Streamer chamber	$\pi^- p \to K_S K_S n$	6, 7	5,100
Zurich, CERN, Imperial College	2	Optical spark chambers	$\pi^- p \to K_S K_S n$	8.9	6,400
Argonne (Effective Mass Spectrometer Group)	3,4,5	Wire spark chambers	$\pi^- p \to K^- K^+ n$ $\pi^+ n \to K^- K^+ p$	6 6	110,000 50,000

The allowed quantum numbers for $K\bar{K}$ states are in the series $J^{PC} = 0^{++}$, 1^{--}, 2^{++}, 3^{--}, ... $K_S K_S$ states have further restrictions on their quantum numbers since J must be even for these states. The isotopic spin I of the $K\bar{K}$ system can be either 0 or 1 with G-parity = $(-1)^{I+J}$. If we define $A_0(A_1)$ to be the amplitude for producing an I = 0 (I = 1) $K^- K^+$ system in the reaction

*Work supported by the U.S. Energy Research and Development Administration.

Invited talk presented at the Fifth International Conference on Experimental Meson Spectroscopy, Northeastern University, Boston, MA., April 1977.

$\pi^- p \to K^- K^+ n$ then the total amplitude for this reaction is $A(\pi^- p \to K^- K^+ n) = A_0 + A_1$, while $A(\pi^- p \to \bar{K}^0 K^0 n) = A(\pi^+ n \to K^- K^+ p) = A_0 - A_1$. Note further that $A(\pi^- p \to \bar{K}^0 K^0 n) = A(\pi^- p \to K_S K_S n) + A(\pi^- p \to K_L K_L n) + A(\pi^- p \to K_S K_L n)$, where the the first and second terms only receive contributions from even-spin $K\bar{K}$ states, while the last term contains only the odd-spin $K\bar{K}$ states. Studying $K\bar{K}$ production using both p and n targets as was done in Ref. 3 allows a separation of the produced $K\bar{K}$ system into its I = 0 and I = 1 components.[6]

DATA

We show in Fig. 1 the $K_S K_S$ effective mass (M_{KK}) distribution from the Notre Dame-Argonne streamer chamber experiment on the reaction[1]

$$\pi^- p \to K_S K_S n \quad . \tag{1}$$

The prominent features of this distribution are the S^* enhancement near threshold and the broad peak in the f-A_2 mass region at ~1300 MeV. Figure 1 also shows the unnormalized t-channel spherical harmonic moments for $|t| < 0.2$ GeV^2 (t is the four-momentum transfer from the π^- to the $K_S K_S$ system). The most prominent feature of the moments of Fig. 1 is the negative excursion of $\langle Y_2^0 \rangle$ at ~1200 MeV followed by a rapid increase.

Ignoring amplitudes with angular momentum $\ell \geq 4$ and helicity $m \geq 2$, the possible $K_S K_S$ amplitudes are S_0, D_0, D_+, D_-; the notation used is L_m with L = S, P, D, ... for $K\bar{K}$ states of spins 0, 1, 2, ..., m = 0 for helicity-0 $K\bar{K}$ states and m = +(-) for helicity-1 $K\bar{K}$ states produced by natural (unnatural) parity exchange The $K_S K_S$ moments are given in terms of the production

Table II. The moments $\sigma\langle Y_\ell^m \rangle \equiv \sqrt{4\pi}\, \frac{d^2\sigma}{dt dM_{KK}} \langle Y_m^\ell \rangle$ in terms of the production amplitudes for the reaction $\pi^- p \to K_S K_S n$

$$\sigma\langle Y_0^0 \rangle = |S_o|^2 + |D_o|^2 + |D_-|^2 + |D_+|^2$$

$$\sigma\langle Y_2^0 \rangle = 2\,\mathrm{Re}\,(D_o^* S_o) + 0.639\,|D_o|^2 + 0.319\,(|D_-|^2 + |D_+|^2)$$

$$\sigma\langle Y_2^1 \rangle = 1.414\,\mathrm{Re}(D_-^* S_o) + 0.452\,\mathrm{Re}\,(D_-^* D_o)$$

$$\sigma\langle Y_2^2 \rangle = 0.391\,(|D_-|^2 - |D_+|^2)$$

$$\sigma\langle Y_4^0 \rangle = 0.857\,|D_o|^2 - 0.571\,(|D_-|^2 + |D_+|^2)$$

$$\sigma\langle Y_4^1 \rangle = 1.107\,\mathrm{Re}\,(D_-^* D_o)$$

$$\sigma\langle Y_4^2 \rangle = 0.452\,(|D_-|^2 - |D_+|^2)$$

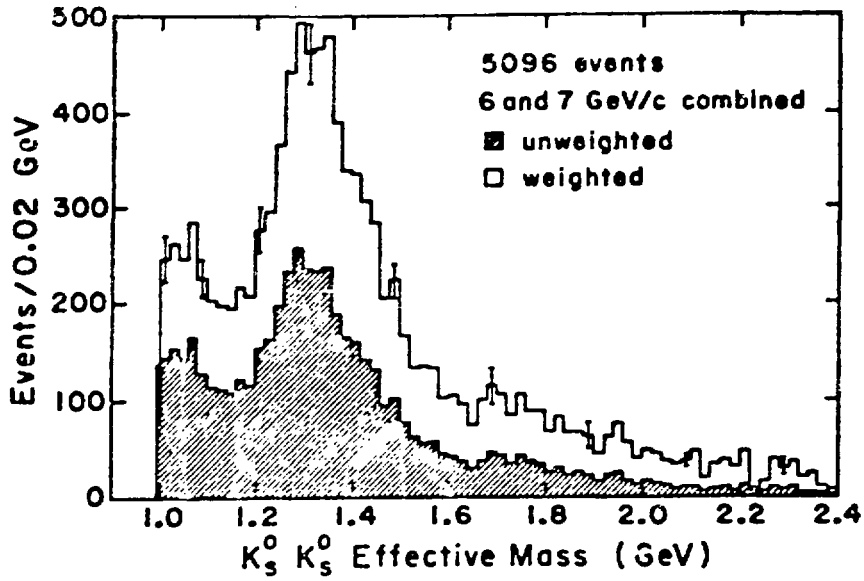

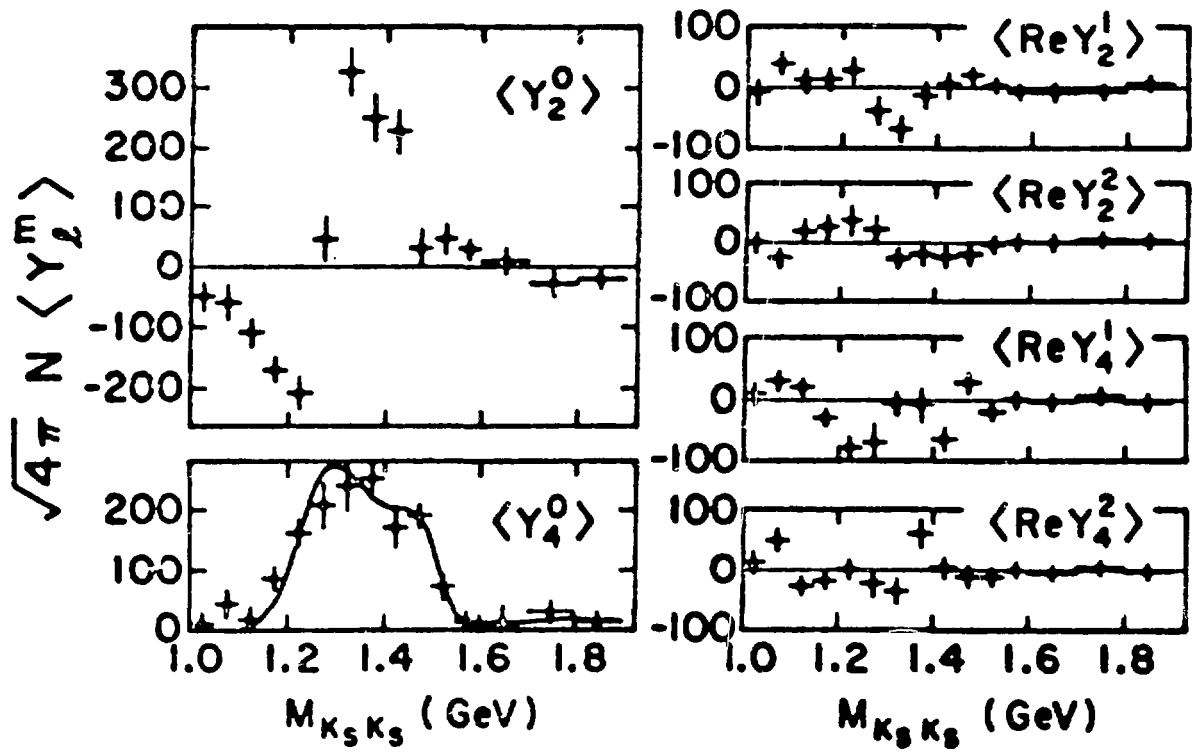

Fig. 1. Unnormalized moments for $\pi^- p \to K_S K_S n$ at 6 and 7 GeV/c as a function of M_{KK} for $|t| \leq 0.2$ GeV^2. The smooth curve on $\langle Y_4^0 \rangle$ is a result of a fit of this moment to f-f' interference.

amplitudes in Table II. The only possible negative contribution to $\langle Y_2^0 \rangle$ comes from interference between the S_o and D_o amplitudes. Thus the behavior of $\langle Y_2^0 \rangle$ indicates the presence of a significant S wave in the 1200-1400 MeV mass region. Cason et al. have proceeded to perform an energy independent amplitude analysis of the $K_S K_S$ system. They have assumed that the amplitudes are nucleon-spin coherent and that D_- and D_o are phase coherent. They then fitted the expressions of Table II to obtain the magnitudes of S_o, D_o, D_-, and D_+ and the absolute value of the S_o-D_o phase difference, $|\varphi_S - \varphi_D|$, as functions of $K_S K_S$ mass. The results of the amplitude analysis are shown in Fig. 2. The S-wave intensity is large at threshold (the S^*), decreases, and has a second peak near 1270 MeV, suggesting the presence of a new S-wave resonance. D_o is large in the f mass region. Motivated by a detailed study of $\langle Y_4^0 \rangle$ in terms of interfering f, A_2, and f' resonances carried out by the Argonne Effective Mass Spectrometer Group,[7] Cason et al. fitted their $\langle Y_4^0 \rangle$ to interfering f and f' resonances (the A_2 is unimportant at small t) to obtain the D-wave phase, φ_D, shown in Fig. 2. (The result of this fit is shown on the $\langle Y_4^0 \rangle$ distribution of Fig. 1.) Using this value of φ_D they obtained the two solutions for φ_S shown in Fig. 2. They noted that solution 1 exhibits a Breit-Wigner phase variation, while solution 2 is slowly varying with no obvious structure. The curve shown on solution 1 is the result of a least-squares fit of this solution for φ_S to a Breit-Wigner and yields the resonance parameters $M = 1255 \pm 5$ MeV and $\Gamma = 79 \pm 10$ MeV. Although there is no a priori reason to rule out solution 2, the authors concluded on the basis of the S-wave intensity variation and the Breit-Wigner phase behavior of solution 1 that they had observed a new scalar meson ($J^{PC} = 0^{++}$).

Cason et al. proceeded to perform the amplitude analysis as a function of t. The S-wave intensity still shows a large enhancement for $0.2 < |t| < 0.5$ GeV^2 (Fig. 3). The t distributions for $|S_o|^2$ and $|D_o|^2$ are also shown in Fig. 3. The slope of the t distribution for $|D_o|^2$ is 11.9 ± 1.2 GeV^{-2}, consistent with one-pion exchange (OPE) as expected for f production, but for $|S_o|^2$ it is 3.7 ± 0.8 GeV^{-2}. They concluded that the new S-wave resonance is not produced dominantly by OPE, and is therefore most likely $I^G = 1^-$. It should be noted that at large $|t|$ the coherence assumptions of the amplitude analysis are less likely to be valid. These assumptions are valid in a region where OPE dominates; however, at large $|t|$, A_2 production becomes important, making the validity of the amplitude analysis at large $|t|$ uncertain. Furthermore, the presence of interfering I = 0 and I = 1 S waves[3] makes the slope of the S-wave cross section observed in this experiment difficult to interpret.

The Zurich-CERN-Imperial College experiment of Wetzel et al.[2] also studied the reaction $\pi^- p \to K_S K_S n$. Their $\langle Y_2^0 \rangle$ moment (Fig. 4) shows the striking S_o-D_o interference pattern observed by Cason et al. A comparison of all the moments from the two experiments shows excellent agreement. The authors performed an amplitude analysis based on OPE with absorption, and the results of this analysis are also shown in Fig. 4. The S-wave intensity, $|S_o|^2$, from this experiment does not show the enhancement at 1270 MeV seen by Cason et al. A detailed comparison of $|S_o|^2$, $|D_o|^2$, and $|\varphi_S - \varphi_D|$

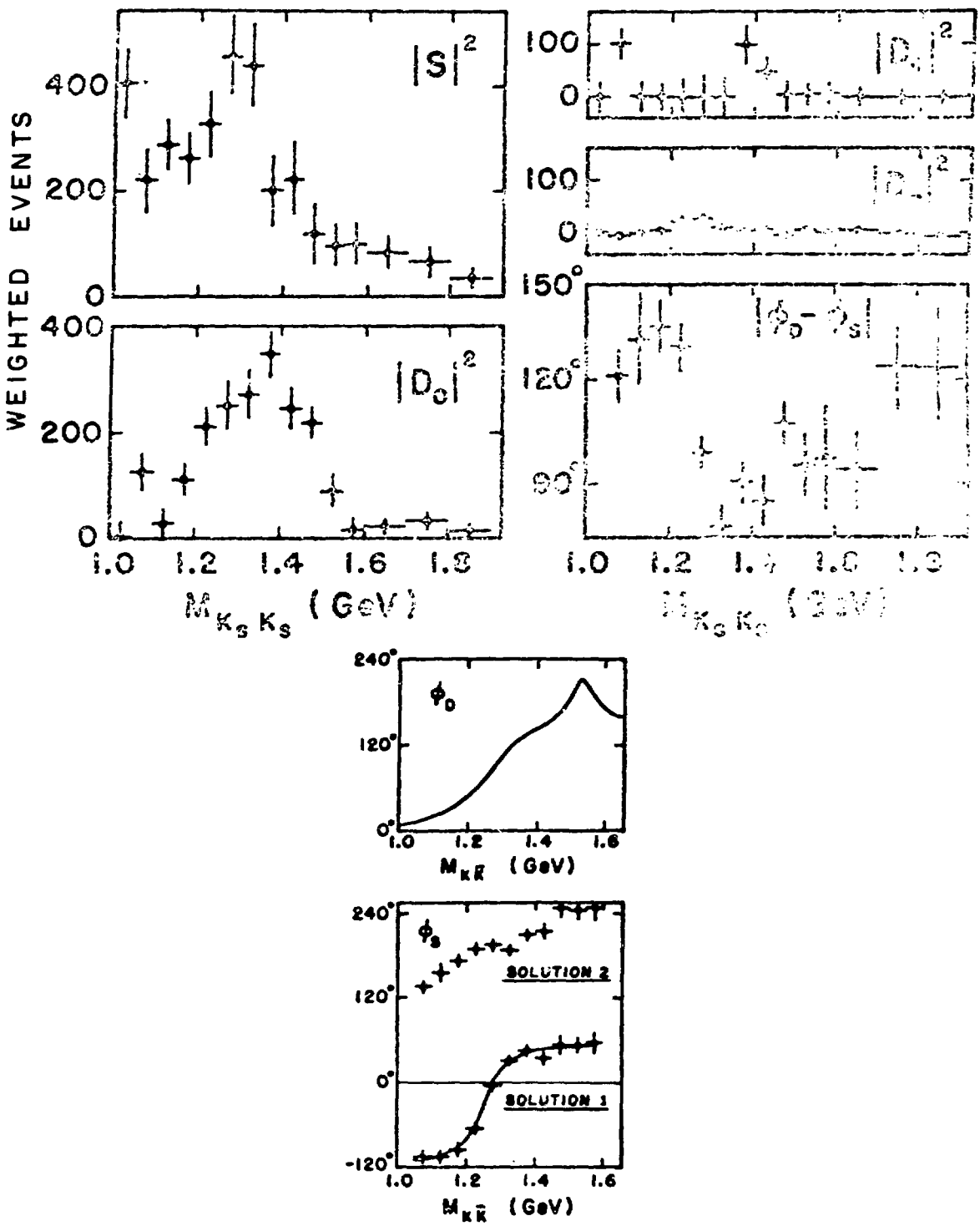

Fig. 2. Results of the amplitude analysis of the $K_S K_S$ system for $|t| \leq 0.2$ GeV^2. The D-wave phase, φ_D, comes from the f-f' fit to $\langle Y_4^0 \rangle$. The curve on solution 1 of φ_S is the result of a Breit-Wigner fit.

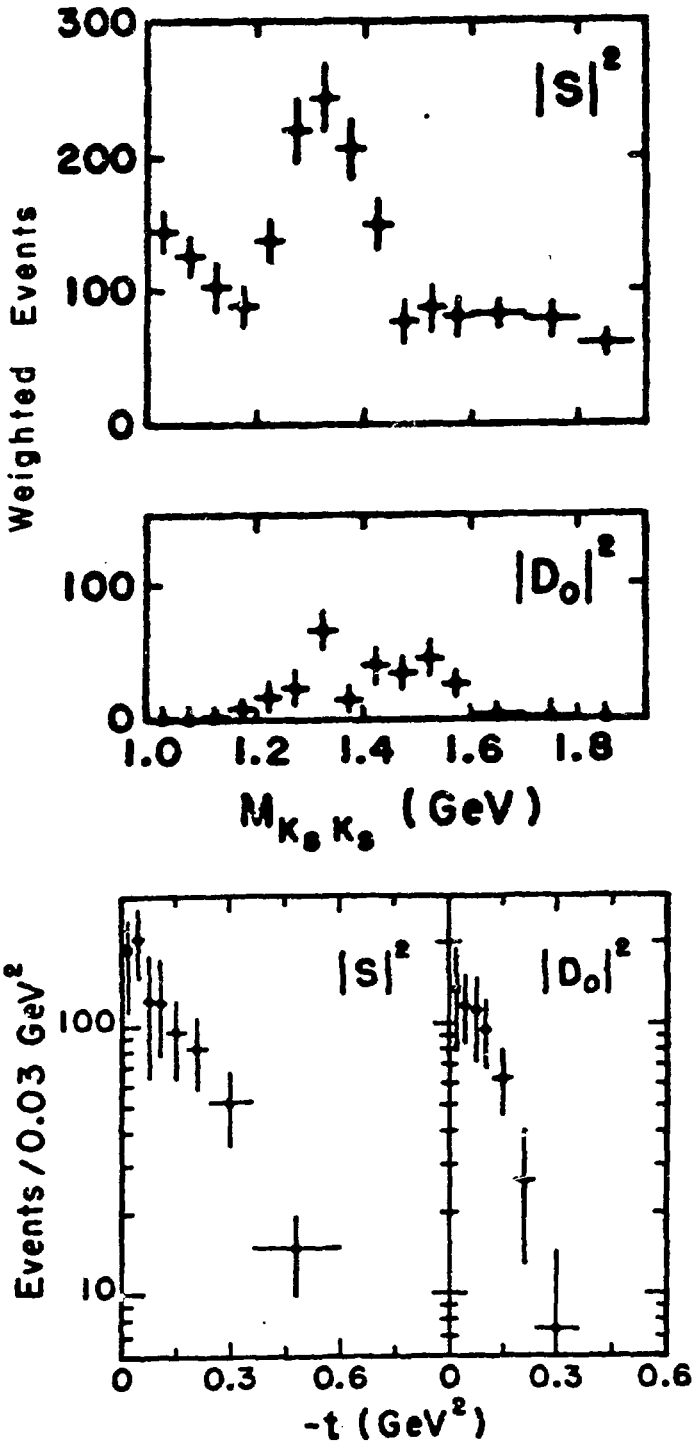

Fig. 3. Results of the amplitude analysis of the $K_S K_S$ system for $0.2 < |t| < 0.5$ GeV^2, and $|S|^2$ and $|D_0|^2$ as a function of t for 1.22 GeV $< M_{KK} <$ 1.32 GeV.

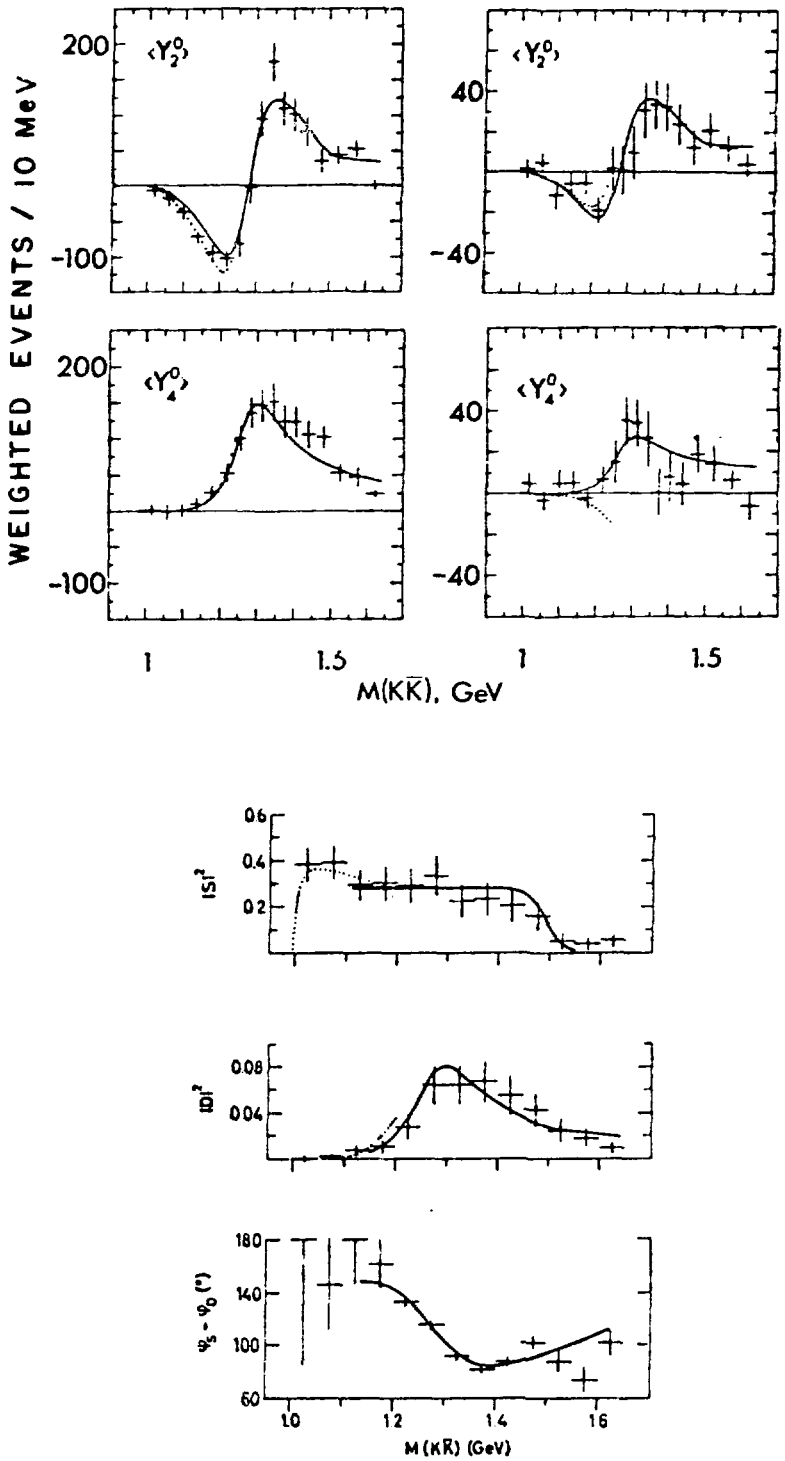

Fig. 4. Unnormalized $\langle Y_2^0 \rangle$ and $\langle Y_4^0 \rangle$ moments and amplitude analysis results for $\pi^- p \to K_S K_S n$ at 8.9 GeV/c. The moments on the left are for $|t| < 0.2$ GeV^2, while those on the right are for $0.2 < |t| < 0.5$ GeV^2. For a discussion of the curves see Ref. 2.

from the two experiments shows, within statistics, excellent agreement. Wetzel et al. concluded that "the peaking in the S-wave observed by Cason et al. may therefore be considered as a statistical fluctuation."

As shown in Table I, the Argonne Effective Mass Spectrometer (EMS) experiment has greater statistics than the two experiments discussed above, and furthermore, studies $K\bar{K}$ production in both the reactions

$$\pi^- p \to K^- K^+ n \tag{2}$$

and

$$\pi^+ n \to K^- K^+ p \quad , \tag{3}$$

to allow a separation of the $K\bar{K}$ system into its $I=0$ and $I=1$ components as discussed above. In addition to the S_o, D_o, D_+, and D_- amplitudes, P_o, P_+, and P_- are now allowed. While having P waves present can lead to additional ambiguous solutions compared to the simpler $K_S K_S$ system, as we shall see below the requirement that the P wave behave reasonably, in fact leads to a unique solution for the amplitudes. The assumptions made in the amplitude analysis carried out by the EMS group are based on OPE with absorption. We assume that S_o, P_o and D_o are t-channel nucleon helicity non-flip (nf) with an OPE t dependence, while the $m=1$ amplitudes arise from absorption of the dominant $m=0$ amplitudes. The explicit form for the t-channel amplitudes is:

$$S_o = S_o^{nf} = A_s \frac{\sqrt{-t}}{\mu^2 - t} e^{B_s(t-\mu^2)}$$

$$P_o = P_o^{nf} = A_{P_o} \frac{\sqrt{-t}}{\mu^2 - t} e^{B_{P_o}(t-\mu^2)}$$

$$D_o = D_o^{nf} = A_{D_o} \frac{\sqrt{-t}}{\mu^2 - t} e^{B_{D_o}(\mu^2-t)}$$

$$P_-^{nf} = A_{P_-} \sqrt{\frac{t'}{t}}\, e^{\left(B_{P_-} t' + C_{P_-} t'^2\right)} \qquad P_-^{f} = \sqrt{\frac{t_{min}}{t'}}\, P_-^{nf}$$

$$D_-^{nf} = A_{D_-} \sqrt{\frac{t'}{t}}\, e^{B_{D_-} t'} \qquad D_-^{f} = \sqrt{\frac{t_{min}}{t'}}\, D_-^{nf}$$

In the above expressions $t' = t - t_{min}$ and $\mu^2 = 0.0195\ GeV^2$. The parameters describing the t dependence of the amplitudes (B_{S_o}, B_{P_o}, etc.) were taken from studies of the reaction $\pi^- p \to \pi^- \pi^+ n$.[8] The results are insensitive to reasonable variations of these parameters. Based on the observation that $\langle Y_2^2 \rangle$, $\langle Y_3^2 \rangle$, and $\langle Y_4^2 \rangle$ are ~0 over the mass and t range considered, we further assumed that $P_+ = P_-$ and $D_+ = D_-$. We then proceeded to fit the 9 t-channel moments with $\ell \leq 4$ and $m \leq 1$ to determine $|S_o|$, $|P_o|$, $|D_o|$, $\varphi_P - \varphi_S$, $\varphi_D - \varphi_S$, A_{P_-} and A_{D_-}. This was done for M_{KK} regions of reactions (2) and (3) separately. There are four solutions for these parameters for each mass slice of each reaction; these solutions were found using the method of Barrelet zeros.

In practice, the EMS group did not fit to the usual $\langle Y_\ell^m \rangle$ moments, but rather to so-called $\langle Q_i \rangle$ moments which are linear combinations of the various $\langle Y_\ell^m \rangle$'s that more clearly display the underlying structure of the amplitudes. The $\langle Q_i \rangle$ moments are defined[9] in Fig. 5 where they are shown for reaction (2) for $|t| < 0.08\ GeV^2$ and $M_{KK} < 1600$ MeV along with the results of the fit. The assumed parametrization of the amplitudes clearly provides an excellent description of the experimentally-measured moments. The fits to reaction (3) (not shown) are equally good.

Figure 6 shows the intensities of S_o, P_o, and D_o for reaction (3) for $|t| < 0.08\ GeV^2$ as determined by this amplitude analysis. There are two sets of solutions for S_o and P_o which differ only for $M_{KK} > 1200$ MeV, while D_o, being fixed by $\langle Y_4^0 \rangle$, has only one solution. One set of solutions (solution 1) exhibits an enhancement in S_o at ~1300 MeV along with a small P_o amplitude, while the other solution (solution 2) shows an enhancement in P_o at 1300 MeV along with a small S_o amplitude. The S^* effect near threshold is prominent in the S_o amplitude for both solutions, while D_o shows the expected enhancement in the f region. Recall that, except for the contribution of the amplitudes with ℓ odd, the moments for reactions (1) and (3) should be the same after taking the unobserved $K_L K_L n$ final state into account for reaction (1). So, we can use the $\pi^- p \to K_S K_S n$ data to select the correct solution set for reaction (3). In particular we note that

$$\sqrt{4\pi}\left(\frac{d^2\sigma}{dtdm}\langle Y_2^0\rangle(\pi^+ n \to K^- K^+ p) - 2\,\frac{d^2\sigma}{dtdm}\langle Y_2^0\rangle(\pi^- p \to K_S K_S n)\right) = 0.894\,|P_o|^2 + (m=1\ \text{terms}),$$

where the m = 1 terms are small. The factor of 2 multiplying the $K_S K_S n$ term in the above equation accounts for the $K_L K_L n$ final state. A comparison of $\langle Y_2^0 \rangle$ for reactions (1) and (3) (Fig. 7) clearly rules out the solution with large P_o, leaving the solution with the S-wave enhancement at 1300 MeV and the small P_o amplitude as the correct solution.

The amplitudes for reaction (2) for $|t| < 0.08\ GeV^2$ are shown in Fig. 8. Again there are two sets of solutions, and these are qualitatively similar to the solutions for reaction (3), although the substantial quantitative differences

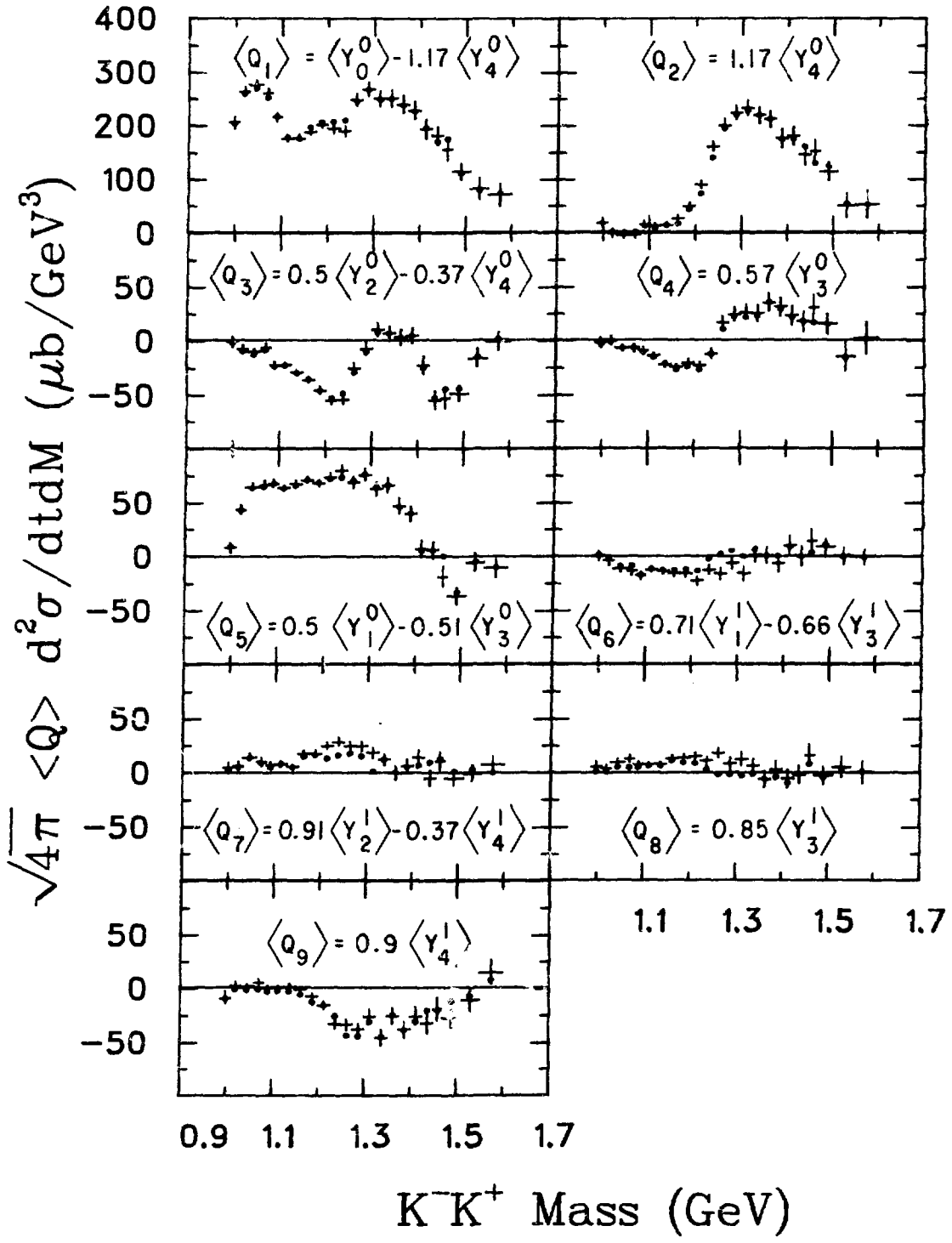

Fig. 5. $\langle Q_i \rangle$ moments for $\pi^- p \to K^- K^+ n$ for $|t| < 0.08$ GeV^2. The dots are the result of the fit discussed in the text. The dominant amplitude contributions to the large moments are $\sigma\langle Q_1 \rangle = |S_0|^2 + |P_0|^2$, $\sigma\langle Q_2 \rangle = |D_0|^2$, $\sigma\langle Q_3 \rangle = S_0 \cdot D_0 + 0.45\,|P_0|^2$, $\sigma\langle Q_4 \rangle = P_0 \cdot D_0$, $\sigma\langle Q_5 \rangle = S_0 \cdot P_0$.

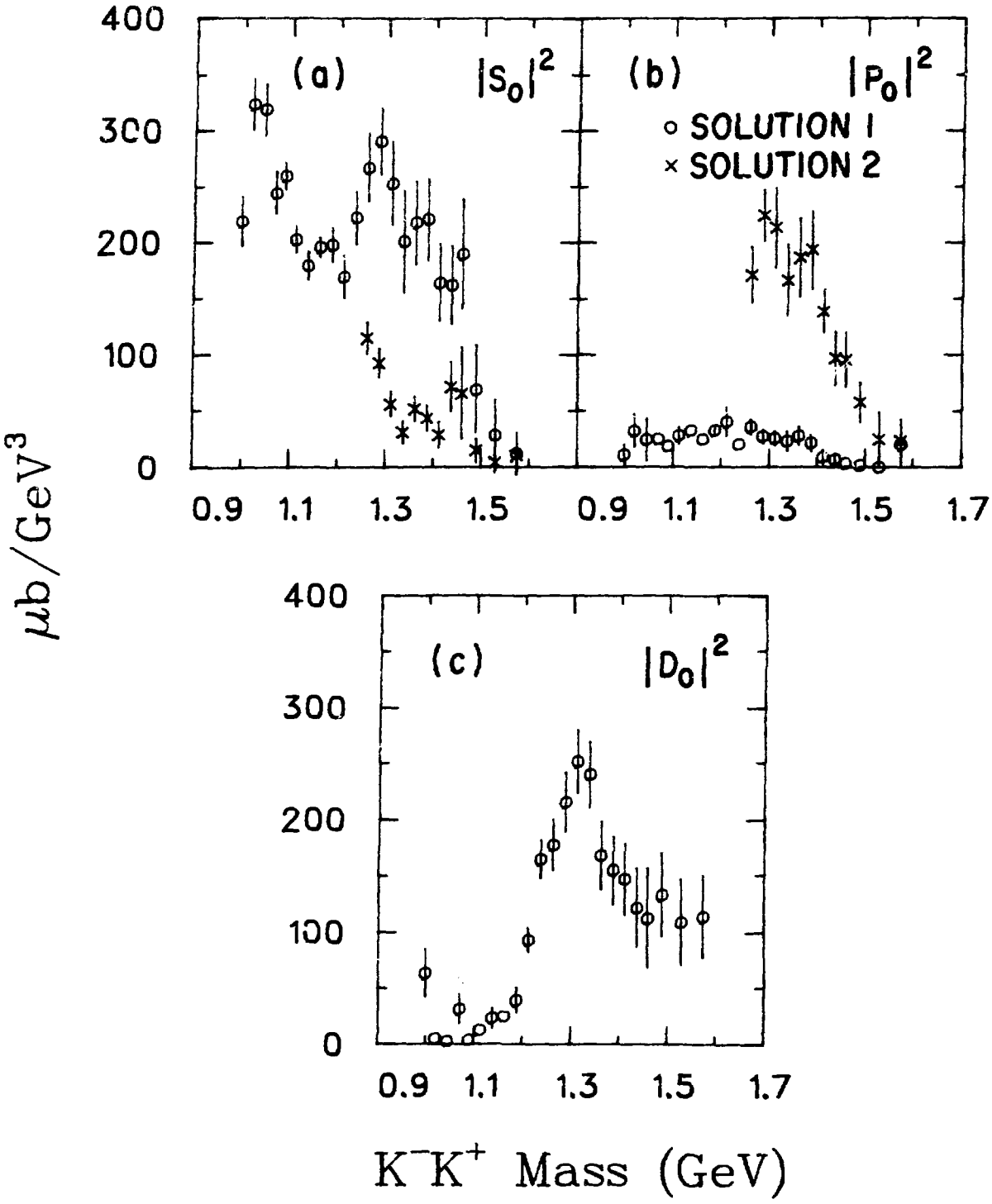

Fig. 6. S_o, P_o, and D_o intensities for $\pi^+ n \to K^- K^+ p$ at 6 GeV/c for $|t| < 0.08$ GeV^2. There are two sets of solutions for S_o and P_o which differ for $M_{KK} > 1.2$ GeV.

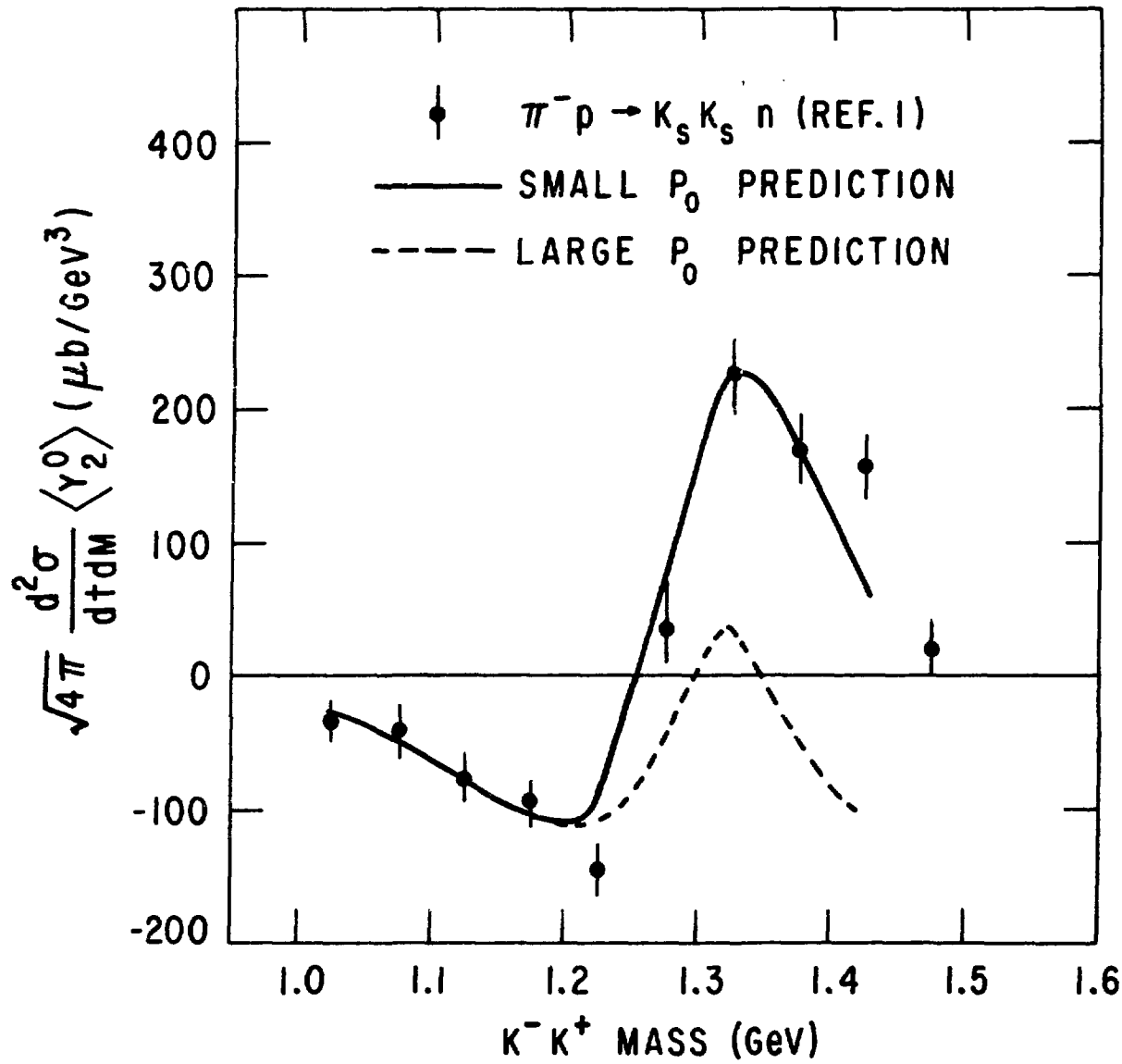

Fig. 7. The $\langle Y_2^0 \rangle$ moment for $\pi^- p \to K_S K_S n$ ($|t| < 0.20$ GeV^2). The $K_S K_S$ data have been normalized to the $\pi^+ n \to K^+ K^- p$ data using the $\langle Y_4^0 \rangle$ moment. The solid curve is the prediction for the $K_S K_S$ $\langle Y_2^0 \rangle$ moment based on the $\langle Y_2^0 \rangle$ moment from $\pi^+ n \to K^- K^+ p$ and assuming the solution with the small P_0 amplitude is correct, while the dashed curve assumes that the large P_0 amplitude is correct.

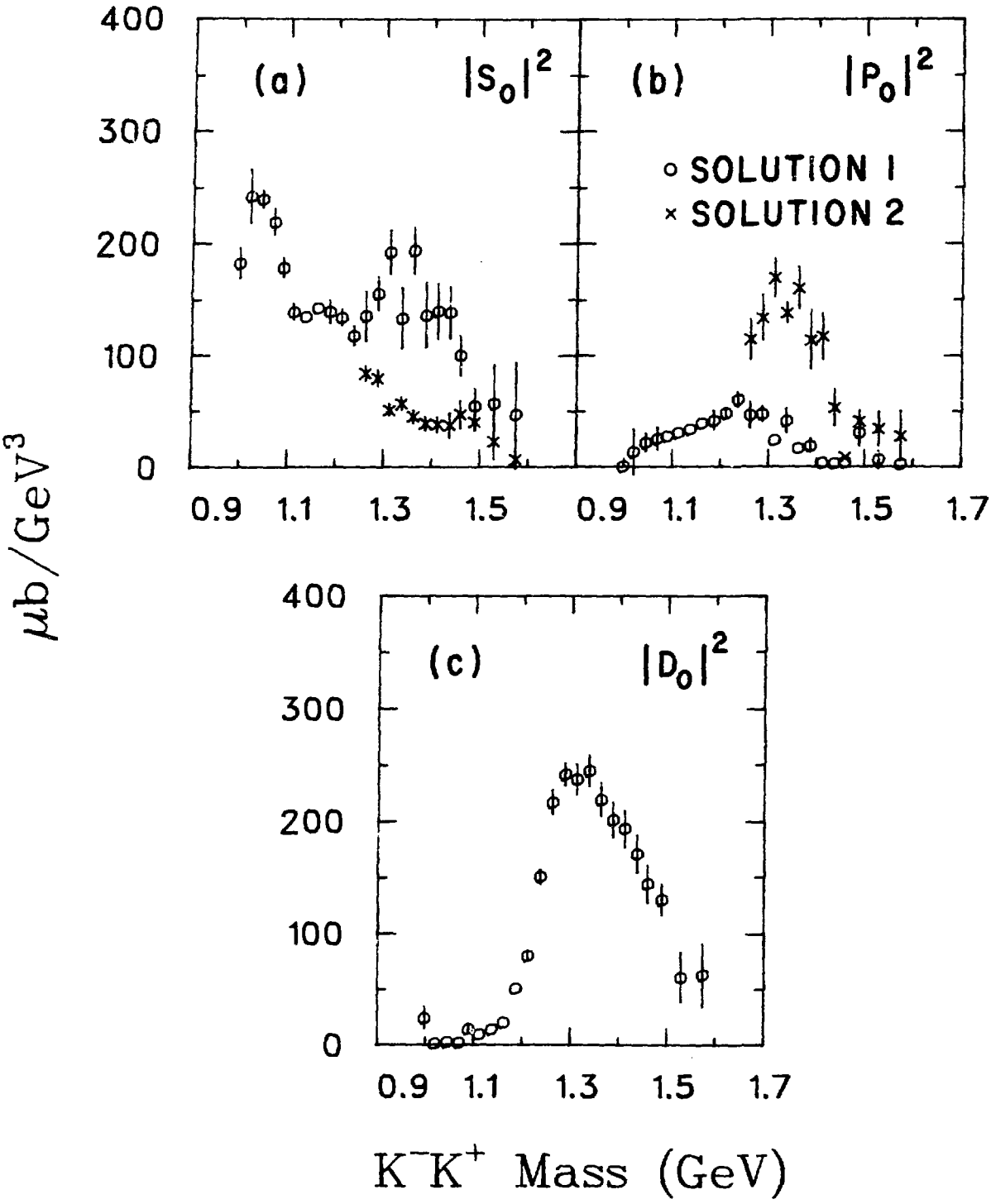

Fig. 8. S_o, P_o, and D_o intensities for $\pi^- p \to K^- K^+ n$ for $|t| < 0.08$ GeV^2.

indicate the presence of interfering I = 0 and I = 1 amplitudes. There are no data presently available that can determine the correct solution set in this case.[10]

The amplitude analysis yields only relative phases, but, as discussed above, the EMS group has carried out detailed fits to $\langle Y_4^0 \rangle$ in terms of interfering f, f' and A_2 resonances[7] which allow one to extract the D-wave phase φ_D, and hence determine the S- and P-wave phases, φ_S and φ_P. Each set of solutions for S_o and P_o gives rise to two sets of solutions for φ_S and φ_P. The two sets of phase solutions for reaction (3) are shown in Fig. 9. The solutions for φ_S are consistent with the two solutions of Cason et al. (see Fig. 2). We note that the solution that exhibits a Breit-Wigner like phase variation for φ_S also has a rapid phase variation for φ_P, while the slowly varying φ_S solution is accompanied by a slowly varying φ_P solution. For reaction (2) there are four sets of phase solutions, and these are shown in Fig. 10.

We are now in a position to extract the I = 0 and I = 1, S-wave and P-wave m = 0 amplitudes. Recall that

$$S_{I=0} = \tfrac{1}{2}(S_{\pi^- p} + S_{\pi^+ p}) \qquad S_{I=1} = \tfrac{1}{2}(S_{\pi^- p} - S_{\pi^+ n})$$

$$P_{I=0} = \tfrac{1}{2}(P_{\pi^- p} + P_{\pi^+ n}) \qquad P_{I=1} = \tfrac{1}{2}(P_{\pi^- p} - P_{\pi^+ n}) \quad .$$

Each combination of a possible solution set for S_o, P_o, φ_S and φ_P from reaction (2) with a solution set from reaction (3) gives one solution for the magnitude and phases of the I = 0 and 1 S-wave and P-wave amplitudes. Since we have four solutions for reaction (2) and two solutions for reaction (3) we obtain eight solutions for the I = 0 and 1 S-wave and P-wave amplitudes. There are, in fact, four unique solutions for the magnitudes of the amplitudes, each of which has two phase solutions. These solutions are shown in Figs. 11 and 12, with Fig. 11 coming from the solution of reaction (2) with the large S_o amplitude at 1300 MeV. Also shown superimposed on the solutions is the behavior expected for the I = 1 P-wave amplitude if it were dominated by the high-mass tail of the ρ meson decaying into $K^- K^+$, with a ρKK coupling given by SU(3).[11] We note that both the magnitude and phase of $P_{I=1}$ for solution I(b) agree extremely well with what is expected from the ρ tail. None of the other solutions agrees with this prediction. The preferred solution I(b) exhibits the S^* effect at threshold and an I = 0 S-wave enhancement at ~1300 MeV, and has a slowly varying I = 0 S-wave phase. $S_{I=1}$ and $P_{I=0}$ are both small in this solution. Solution I(a) has both a rapidly varying $\varphi_S^{I=1}$ and $\varphi_P^{I=0}$. The other solutions (II, III, and IV) have both I = 1 S-wave and I = 0 P-wave enhancements at ~1300 MeV. Thus on the basis of selecting the solution that agrees with that expected for the ρ tail, this analysis has shown that the new S-wave enhancement is I = 0 and has a slowly varying phase.

The EMS group has also carried out the amplitude analysis at larger $|t|$ ($0.2 < |t| < 0.4$ GeV^2), and the resultant S-wave and P-wave intensities

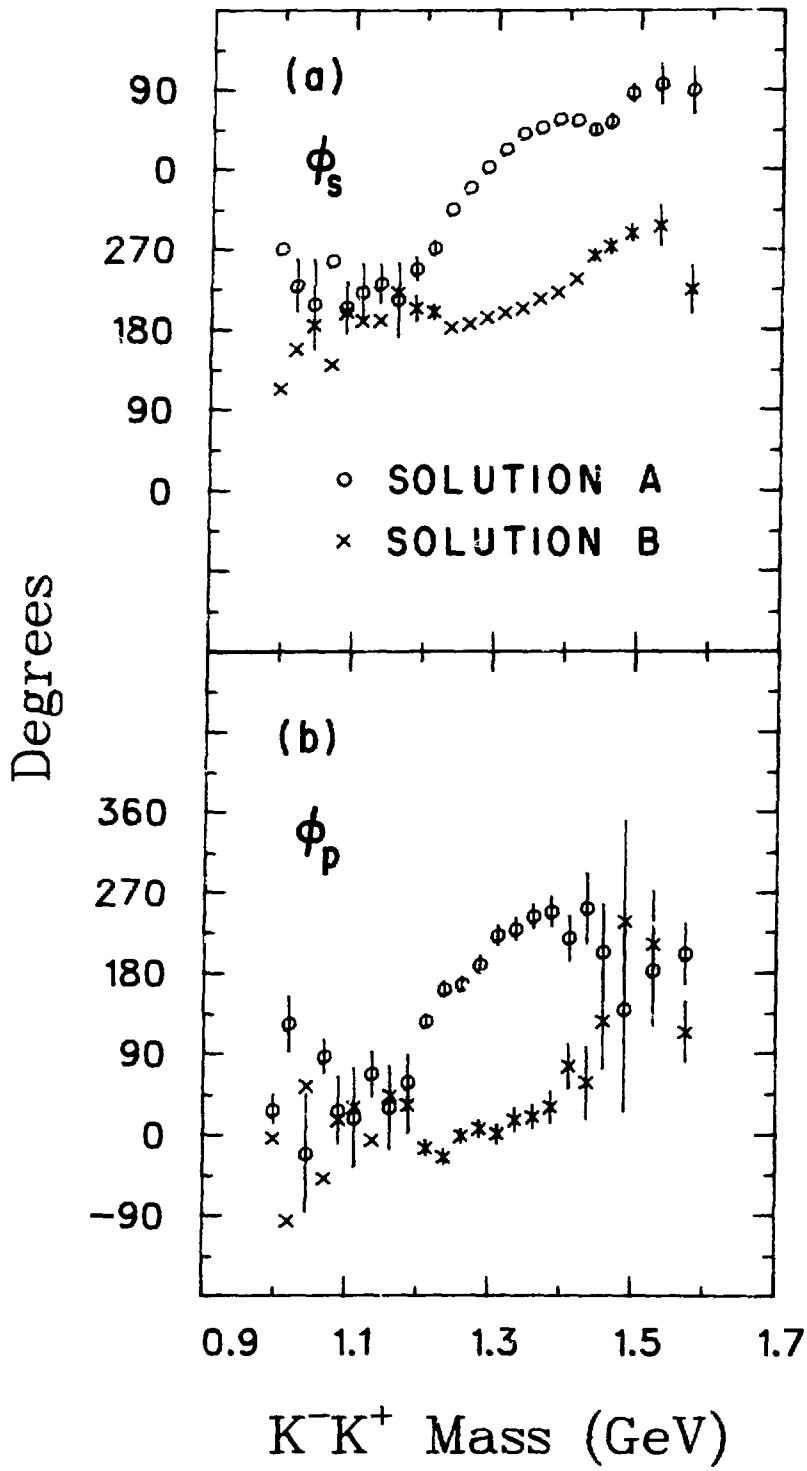

Fig. 9. S-wave and P-wave phases for $\pi^+ n \to K^- K^+ p$ for $|t| < 0.08$ GeV^2. The error bars for both solutions are the same.

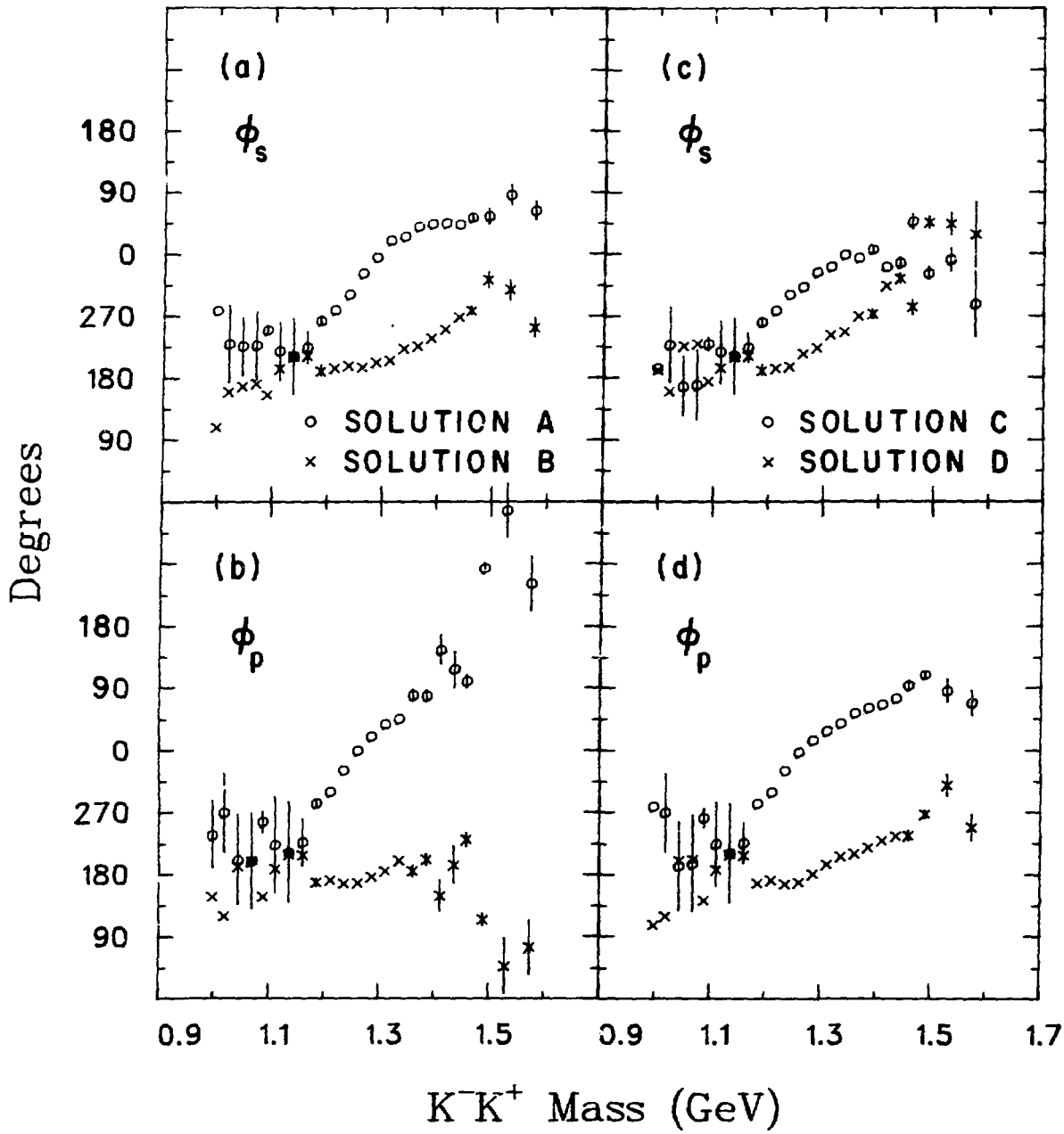

Fig. 10. S-wave and P-wave phases for $\pi^- p \to K^- K^+ n$ for $|t| < 0.08$ GeV^2. Solutions A and B for φ_S and φ_P arise from solution 1 of Fig. 8, while solutions C and D arise from solution 2 of Fig. 8. The error bars for solutions A and B, as well as those for C and D are the same.

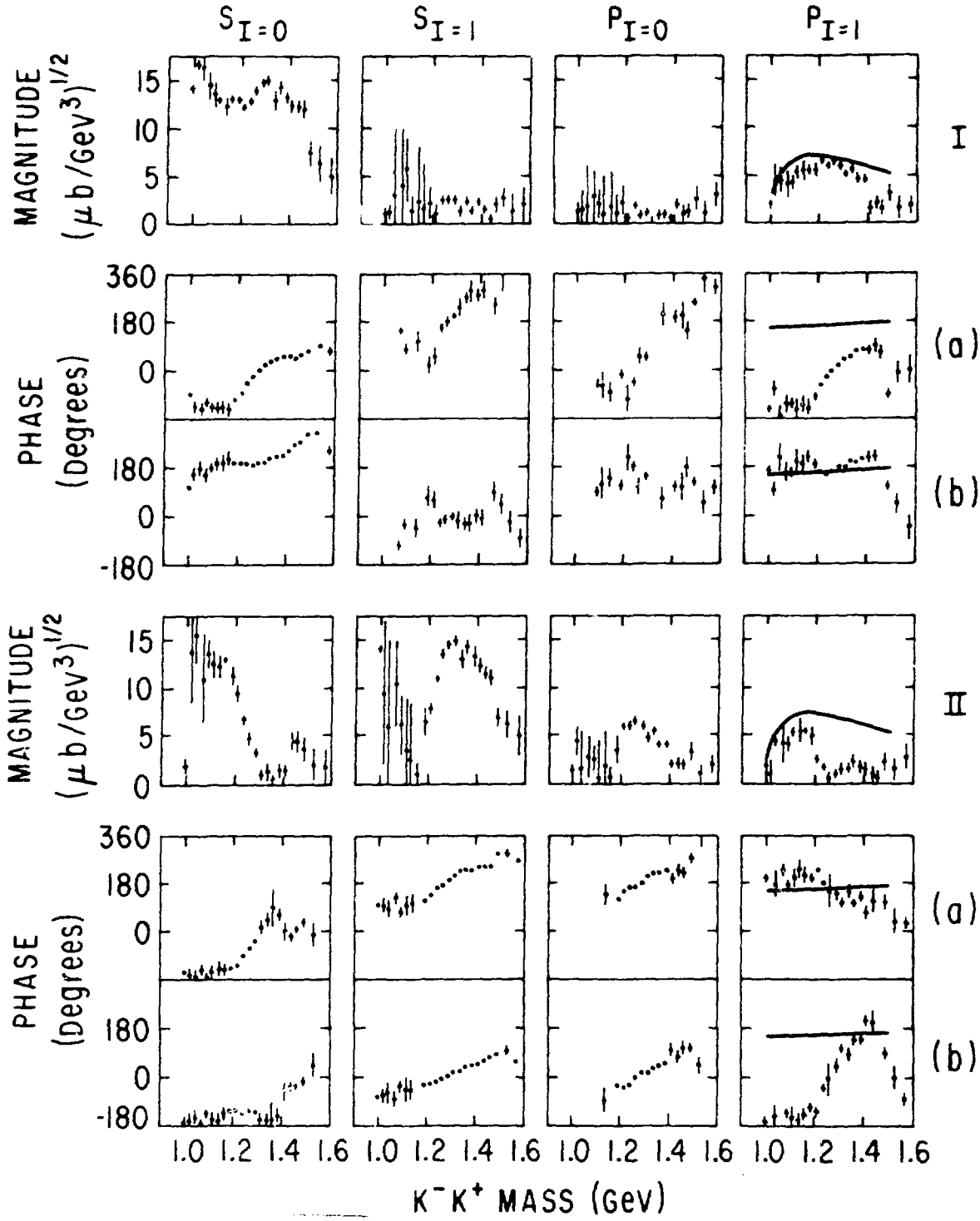

Fig. 11. I = 0 and I = 1 S-wave and P-wave amplitudes for $|t| < 0.08$ GeV^2. These four solutions use the solution for $\pi^- p \to K^- K^+ n$ that has the large S_0 amplitude (solution 1 of Fig. 8). The curves superimposed on $P_{I=1}$ represent the behavior expected for the I = 1 P-wave amplitude if it were dominated by the high mass tail of the ρ meson decaying into $K^- K^+$.

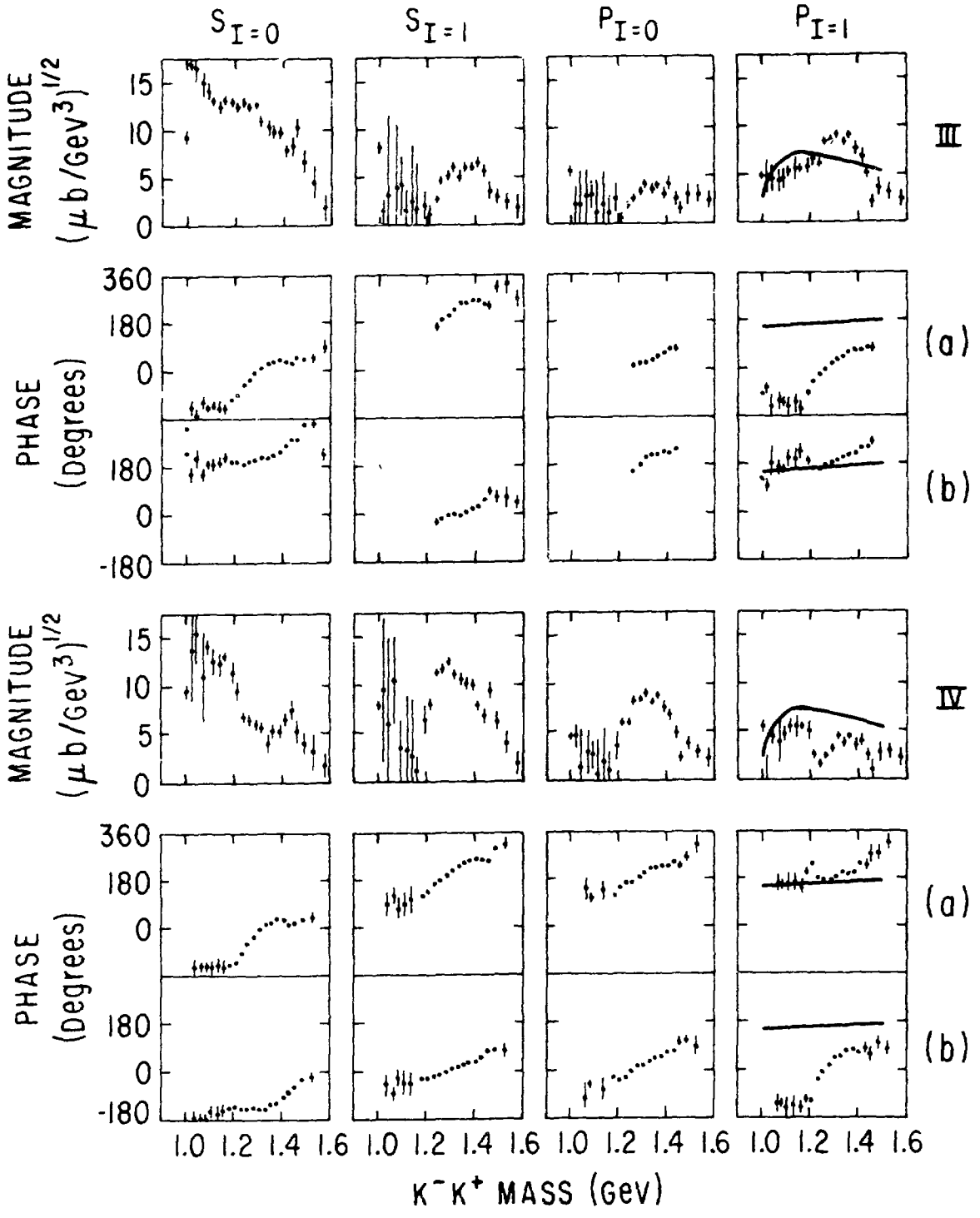

Fig. 12. I = 0 and I = 1 S-wave and P-wave amplitudes for $|t| < 0.08$ GeV^2. These four solutions use the solution for $\pi^- p \to K^- K^+ n$ that has the small S_0 amplitude (solution 2 of Fig. 8). See Fig. 11 for a discussion of the curves.

are shown in Fig. 13. The same caveats apply here as were made in discussing the large $|t|$ analysis of Cason et al. Again, comparison with the data of Cason et al. selects the solution with the large S wave at 1300 MeV and small P wave as being the correct solution for $\pi^+ n \to K^- K^+ p$. The two solutions for $\pi^- p \to K^- K^+ n$ are indistinguishable. No separation of the amplitudes into I = 0 and I = 1 components has been done at large $|t|$, although the large difference between the S-wave intensity for the two reactions indicates the presence of both I = 0 and I = 1 S-wave amplitudes at large $|t|$.

DISCUSSION

The observation of the new I = 0 S-wave state discussed in this review puts the SU(3) classification of the 0^{++} mesons into some doubt. Two years ago Morgan[12] classified the scalar mesons into a non-ideally mixed nonet ($\theta \sim 65^\circ$) comprising the $\delta(975)$, $S^*(993)$, $\kappa(1250)$, and the $\epsilon(1300)$. He was able to obtain a self-consistent set of masses and coupling constants. This classification scheme has difficulty in explaining the new I = 0 S-wave state. The intensity variation in the I = 0 S-wave amplitude can be qualitatively understood as being due to the interference of the $S^*(993)$ with the broad $\epsilon(1300)$; however, this would imply an anomalously large coupling of the ϵ to $K\bar{K}$. In addition, the S-wave enhancement at large t may be indicative of an additional I = 1 S-wave state. The new $\kappa(1450)$ discussed at this conference[13] also does not easily fit into Morgan's classification scheme. Alternative schemes based on the M.I.T. bag model[14] which classify some of the established states as four-quark states have been proposed.

ACKNOWLEDGEMENTS

Special thanks are due to my colleagues at Argonne, D. Ayres, R. Diebold, S. Kramer, A. Pawlicki and A. Wicklund, for their efforts on the EMS experiment. Helpful discussions with N. Cason, W. Fickinger, and V. Polychronakos are gratefully acknowledged.

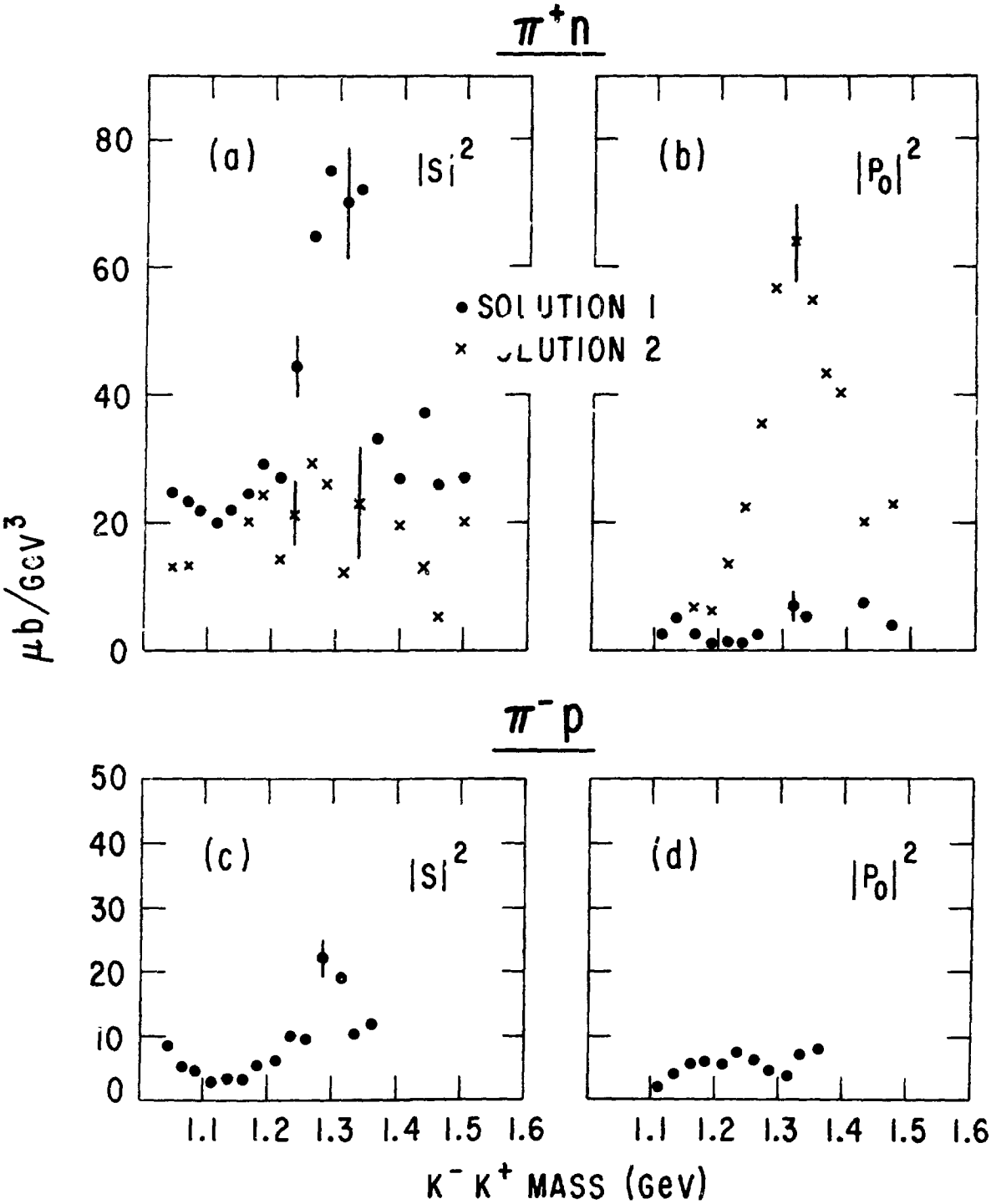

Fig. 13. S_0 and P_{0_2} intensities for $\pi^+ n \to K^- K^+ p$ and $\pi^- p \to K^- K^+ n$ for $0.2 < |t| < 0.4$ GeV^2. Only typical error bars are shown.

REFERENCES

1. N. M. Cason et al., Phys. Rev. Letters 36, 1485 (1976). The data from this experiment for $0.2 < |t| < 0.5$ GeV^2 come from a private communication from N. Cason.
2. W. Wetzel et al., Nucl. Phys. B115, 208 (1976).
3. A. J. Pawlicki et al., Phys. Rev. Letters 37, 1666 (1976).
4. A. J. Pawlicki et al., Phys. Rev. D15, 3196 (1977).
5. D. Cohen et al., to be published.
6. H. J. Lipkin, Phys. Rev. 176, 1709 (1968).
7. A. J. Pawlicki et al., Phys. Rev. Letters 37, 971 (1976).
8. A. D. Martin and C. Michael, Nucl. Phys. B84, 83 (1975); A. B. Wicklund et al., to be published.
9. The K^-K^+ moments are given in terms of the production amplitudes in Table II of Ref. 4.
10. Available bubble chamber data on the reaction $\pi^+ n \to K_S K_S p$ at 6 GeV/c are not sufficiently precise to discriminate between our two solutions (private communication from W. Fickinger).
11. The ρ was parametrized as a relativistic P-wave Breit-Wigner resonance, corrected for K^-K^+ phase space and barrier factors. SU(3) predicts $\frac{g_{\rho K^- K^+}}{g_{\rho \pi^- \pi^+}} = \frac{1}{2}$. See, for example, J. Pisut and M. Roos, Nucl. Phys. B6, 325 (1968); J. D. Jackson, Nuovo Cimento 34, 1644 (1964); A. J. Pawlicki et al., Ref. 4. The normalization was taken from studies of the reaction $\pi^- p \to \rho^0 n$ at 6 GeV/c. See A. B. Wicklund et al., Ref. 8.
12. D. Morgan in New Directions in Hadron Spectroscopy, edited by S. L. Kramer and E. L. Berger (Argonne National Laboratory Report ANL-HEP-CP-75-58, 1975), p. 45; D. Morgan, Phys. Lett. 51B, 71 (1974).
13. P. Estabrooks, these proceedings; D. Leith, these proceedings; P. Estabrooks et al., SLAC-PUB-1886.
14. R. L. Jaffe, Phys. Rev. D15, 267 (1977).